Origin of positive out-of-plane magnetoconductivity in overdoped $Bi_{1.6}Pb_{0.4}Sr_2CaCu_{1.96}Fe_{0.04}O_{8+\delta}$

Takao Watanabe,[1,*] Tomohiro Usui,[1] Shintaro Adachi,[1,†] Yuki Teramoto,[1] Mihaly M. Dobroka,[1] Itsuhiro Kakeya,[2]
Akihiro Kondo,[3] Koichi Kindo,[3] and Shojiro Kimura[4]

[1]*Graduate School of Science and Technology, Hirosaki University, 3 Bunkyo, Hirosaki 036-8561, Japan*

[2]*Department of Electronic Science and Engineering, Kyoto University, Kyoto 615-8510, Japan*

[3]*Institute for Solid State Physics, University of Tokyo, 5-1-5 Kashiwanoha, Kashiwa, Chiba 277-8581, Japan*

[4]*Institute for Materials Research, Tohoku University, 2-1-1 Katahira, Aoba-ku, Sendai 980-8577, Japan*

To elucidate the pseudogap phase diagram including the overdoped state of high transition temperature (high-T_c) cuprates, we must understand the origin of the positive out-of-plane magnetoconductivity observed in these compounds. For this purpose, the out-of-plane resistivity $\rho_c(T,H)$ of an overdoped $Bi_{1.6}Pb_{0.4}Sr_2CaCu_{1.96}Fe_{0.04}O_{8+\delta}$ (Bi-2212) single crystal is measured under pulsed magnetic fields up to 60 T. We show that the superconducting density-of-states depletion effect, in addition to the pseudogap effect, clearly appears below the superconducting fluctuation regime, and the contribution becomes dominant in the superconducting state.

I. INTRODUCTION

To determine the mechanism of high-T_c superconductivity, we must understand the relationship between the pseudogap and superconductivity [1]. To date, different classes of theoretical models for high-T_c superconductivity have proposed different pseudogap phase diagrams [2]. That is, if the pseudogap is a necessary ingredient for pairing, the pseudogap opening temperature T^* may merge with T_c in the overdoped state, whereas if the pseudogap is of a competing order, T^* may cross the T_c "dome" near the optimal doping. The difference especially appears in the overdoped region; hence it is important to investigate this region. However, it is difficult to determine whether the observed effect is related to the pseudogap or the superconductivity when T^* is close to T_c.

It is well known that $\rho_c(T)$ shows a typical upturn [3] and a negative $\rho_c(H)$ slope [4,5] at high fields below T^*. Because ρ_c probes the electronic density-of-states (DOS) around the Fermi level, reflecting the tunneling nature between CuO_2 planes in high-T_c cuprates, the semiconductive upturn in $\rho_c(T)$ is attributed to the decrease of DOS caused by the pseudogap opening, and the negative $\rho_c(H)$ slope is attributed to the DOS recovery along with the suppression of the pseudogap under magnetic fields. These facts are well established, and thus we can usually estimate T^* by the ρ_c behavior.

On the other hand, because superconductivity is also a phenomenon connected to the energy gap, there have been proposals from both experimental [6–8] and theoretical [9,10] points of view that superconductivity causes similar effects on ρ_c in a temperature and magnetic field range in which the DOS effect dominates over the Cooper pair tunneling effect. In such cases, it is difficult to distinguish T^* from the onset temperature of the superconducting fluctuation T_{scf}. However, this interpretation for the superconductivity-originated anomalous ρ_c behavior has not been generally accepted.

To address this issue, we focus on the magnetic field dependence of ρ_c up to high fields, especially in the superconducting fluctuation regime. In general, the pseudogap is less sensitive to magnetic fields than superconductivity [11]. Therefore, if we can obtain a high enough field near the upper critical field H_{c2}, we can expect to observe the pseudogap and superconducting contributions separately for the magnetic field dependence of ρ_c. Hence we measure $\rho_c(T,H)$ of Fe-substituted overdoped Bi-2212 under high pulsed magnetic fields up to 60 T. For comparison, we also measure $\rho_{ab}(T,H)$ of the same sample.

II. EXPERIMENT

Single crystals were grown in air using the traveling-solvent floating zone (TSFZ) method. The Bi site was partially substituted by Pb to overdope the sample. The Cu site was also substituted by 2% Fe to reduce T_c. The crystals were annealed under flowing oxygen at 400 °C for 50 h to promote hole doping ($T_c = 50$ K, $p = 0.22$). In this study, T_c was determined by the onset of zero resistivity. The doping level (p) was obtained using the empirical relation [12] with maximum $T_c = 71$ K for this sample.

The in-plane resistivity $\rho_{ab}(T,H)$ as well as the $\rho_c(T,H)$ measurements were performed using the dc four-terminal method [13]. Two types of magnets were used: the magnet at the Institute for Materials Research (IMR), Tohoku University, which provides steady magnetic fields up to 17.5 T, and the nondestructive pulsed magnet at the Institute for Solid State Physics (ISSP), University of Tokyo, which provides pulsed magnetic fields (36-ms pulse duration) up to 60 T. Magnetic fields were applied parallel to the c axis. In the pulsed magnet measurements, we did not observe hysteresis behavior in high magnetic fields above the peak field H_{peak} at which $\rho_c(H)$ is maximum. Furthermore, all down-ramped data coincided for measurements under several maximal fields, suggesting that the data were obtained with minimal eddy current influence.

In the following section, we will first estimate T^* and T_{scf} of this sample using the temperature dependence of ρ_c and ρ_{ab}, respectively. Then, we will show that the out-of-plane magnetoconductivity (MC) is composed of two positive components below T_{scf}. This two component analysis enables us to estimate H_{c2} at several temperatures. We will also estimate H_{c2} from the magnetic field dependence of ρ_{ab} in a standard manner. Consequently, an experimental H–T phase

---
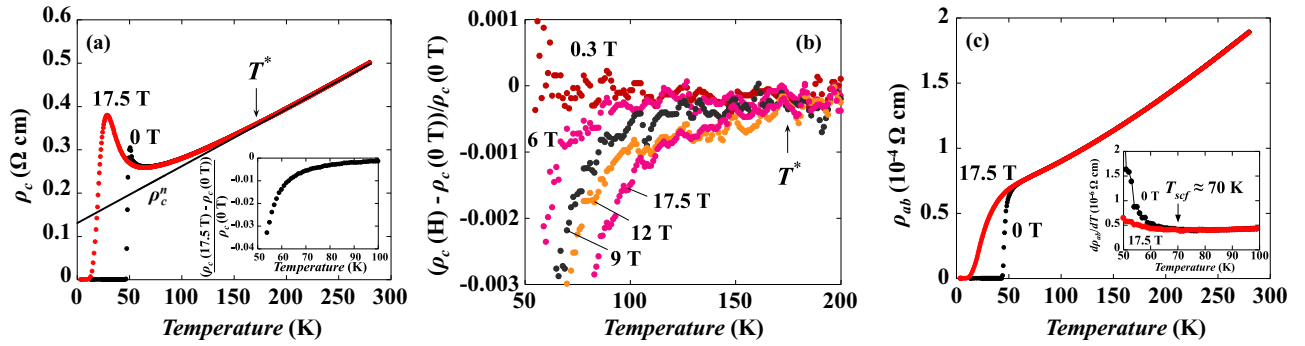
FIG. 1. (a) Out-of-plane resistivity $\rho_c(T)$ for $Bi_{1.6}Pb_{0.4}Sr_2CaCu_{1.96}Fe_{0.04}O_{8+\delta}$ with and without a 17.5-T magnetic field. Here, ρ_c^n is a linear extrapolation of $\rho_c(T)$ at higher temperatures. The arrow indicates the pseudogap opening temperature $T^* \approx 166$ K. The inset shows the negative magnetoresistance (MR) on ρ_c under 17.5 T. (b) Temperature dependence of the out-of-plane MR under several fields. (c) In-plane resistivity $\rho_{ab}(T)$ with and without a 17.5-T magnetic field. The inset shows the temperature dependence of $d\rho_{ab}/dT$. The arrow indicates the onset temperature of the superconducting fluctuation $T_{scf} \approx 70$ K.

diagram of this compound will be used to validate the analysis. Finally, we will discuss the implications of the obtained results for the pseudogap phase diagram.

III. RESULTS AND DISCUSSION

Figure 1(a) shows $\rho_c(T)$ for a $Bi_{1.6}Pb_{0.4}Sr_2CaCu_{1.96}Fe_{0.04}$ $O_{8+\delta}$ crystal with and without a steady 17.5-T magnetic field. For zero field, $\rho_c(T)$ is metallic $[d\rho_c(T)/dT > 0]$ over a wide temperature region, showing a slight upward trend with decreasing temperature. From this result, we estimate the pseudogap opening temperature T^* to be 166 K. Here, T^* is defined as the temperature at which ρ_c increases by 1% from that for high-temperature linear behavior [3,13,14].

Figure 1(b) shows the temperature dependence of the out-of-plane magnetoresistance (MR) for several magnetic fields H. A small negative MR is observed below 170 K, and the magnitude increases with increasing magnetic field. This negative MR confirms that the pseudogap opens below this temperature [4,7]. However, for a zero field, $\rho_c(T)$ shows a steep increase near T_c [Fig. 1(a)]. When a 17.5-T magnetic field is applied, $\rho_c(T)$ increases below T_c, showing a sharp maximum around 30 K and then decreases to zero [Fig. 1(a)]. The inset of Fig. 1(a) shows an enlarged view of the out-of-plane MR at 17.5 T. The small negative MR starting below T^* rapidly increases near T_c. These results suggest that the superconducting DOS fluctuation effect is added to the pseudogap effect below the onset temperature of the superconducting fluctuation T_{scf} [13].

To estimate T_{scf}, $\rho_{ab}(T)$ was measured with and without a steady 17.5-T magnetic field [Fig. 1(c)]. The upward curvature for the temperature dependence is evident, further indicating that the sample is in an overdoped state [13,14]. However, a small negative MR, whose origin is unknown, was observed above T_c (details will be published elsewhere). Therefore, to estimate T_{scf}, we cannot use our standard method of determining the onset temperature for the rapid increase of positive MR [13]. Instead, the temperature derivative $d\rho_{ab}/dT$ is compared for a zero field and a 17.5-T field [inset of Fig. 1(c)]. The difference in $d\rho_{ab}/dT$ appears below 70–75 K. Because the Aslamazov-Larkin (AL)-type superconducting

fluctuation effect (paraconductivity) is expected to affect the slope of $\rho_{ab}(T)$ below T_{scf}, the onset temperature for the change may be assigned as T_{scf}. Note that T^* is far greater than T_{scf}, even in this overdoped state ($p = 0.22$) [15].

Figure 2(a) shows the high pulsed magnetic field data for $\rho_c(H)$ above and below T_c. At 1.4 K, $\rho_c(H)$ remains at zero up to 55 T, indicating that H_{c2} is above 55 T. At other temperatures below T_c, $\rho_c(H)$ shows a typical peak structure; it changes from zero to a resistive state at a vortex melting field, H_m, reaching a maximum at H_{peak} before decreasing to a constant value. This peak structure in $\rho_c(H)$ can be understood by parallel two-channel tunneling conductivity [8]: Cooper pair tunneling, $\sigma_c^{Cooper}(H)$, and quasiparticle tunneling, $\sigma_c^{qp}(H)$. That is, $\rho_c(H) = 1/[\sigma_c^{Cooper}(H) + \sigma_c^{qp}(H)]$. The behavior under weak magnetic fields is controlled by $\sigma_c^{Cooper}(H)$, which arises due to phase slips between neighboring CuO_2 planes caused by the motion of mobile pancake vortices, and the Josephson contribution decreases with increasing field strength [17]. However, $\sigma_c^{qp}(H)$ increases under high magnetic fields, causing a negative $\rho_c(H)$ slope, and H_{peak} is a crossover field for both contributions. In the following section, we concentrate on the analysis of the negative $\rho_c(H)$ slope.

We consider $\sigma_c(H)$ above T_c. Figures 2(b) and 2(c) show the MC, $\Delta\sigma_c(H) = \sigma_c(H) - \sigma_c(0)$, as a function of H^2, at 50 and 60 K, respectively. Above 65 K, we additionally measure the MC using a steady magnet up to 16 T [Fig. 2(d)]. The MC rapidly increases with increasing magnetic field, approaching $\propto H^2$ for higher fields. With increasing temperature, the field interval MC, which follows $\propto H^2$, extends to lower fields, and the slope, a, decreases. These data imply that the MC comprises two positive components: one component gradually increases with aH^2 (hereafter, we denote this component as $\Delta\sigma_c^{PG}$), and the other component rapidly increases with increasing magnetic field but tends to saturate at higher fields (hereafter, we denote this component as $\Delta\sigma_c^{SC-DOS}$). This two component analysis is schematically shown in Fig. 2(e). Figure 2(d) shows that the H^2 component, $\Delta\sigma_c^{PG}$, is present both below and above T_{scf}, while the component with a different (faster) H dependence, $\Delta\sigma_c^{SC-DOS}$, decreases with increasing temperature and vanishes around T_{scf} ($=75$ K). Thus the former component ($\Delta\sigma_c^{PG}$) is attributed to the pseudogap
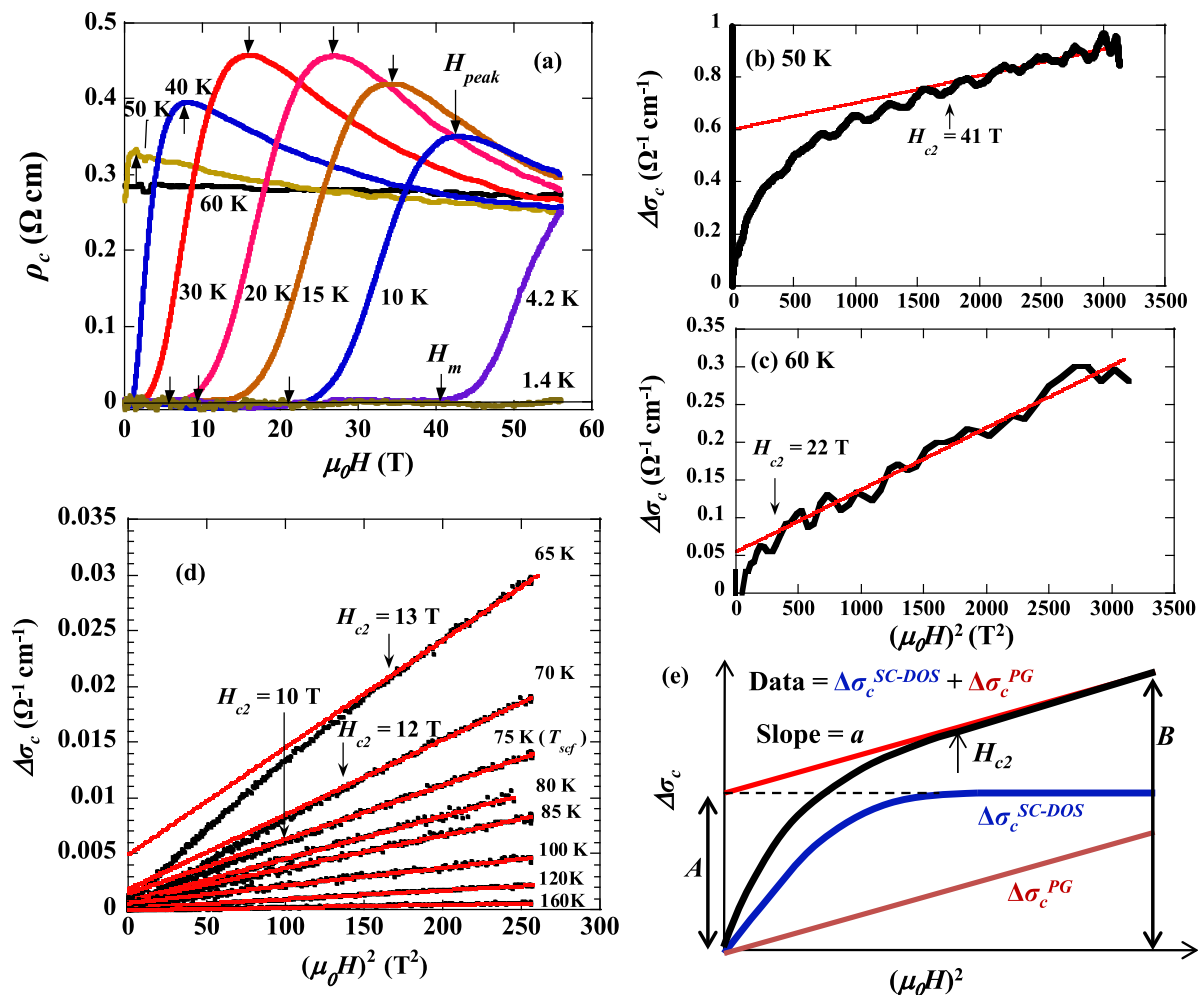
FIG. 2. (a) Magnetic field dependence of ρ_c for $Bi_{1.6}Pb_{0.4}Sr_2CaCu_{1.96}Fe_{0.04}O_{8+\delta}$ below and above T_c. The arrows indicate the peak field H_{peak}, and the vortex melting field H_m (H_m is defined as a field in which $\rho_c = 0.01\rho_c^n$ [16]). (b), (c) Out-of-plane magnetoconductivity (MC), $\sigma_c(H)-\sigma_c(0\,T)$, at 50 and 60 K, respectively. In (b), the normal state $\sigma_c(0\,T)$ was assumed as an extrapolated value to the zero field of the high-field data. (d) Out-of-plane MC above 65 K for steady magnetic fields. (b)–(d) The solid lines are linear extrapolations of MC at higher fields. Here, H_{c2} is defined as the field at which MC deviates 1% as an average from these lines. (e) Schematic representation for the two component analysis used above T_c.

effect, and the latter component ($\Delta\sigma_c^{SC-DOS}$) is attributed to the superconducting DOS depletion effect. This result verifies that the positive superconducting contribution in MC appears below T_{scf}. Furthermore, the observation of H^2 MC at high temperatures above T_{scf} (when superconducting fluctuations are presumably gone) justifies the following analysis in Figs. 2(b)–2(d), which separate the pseudogap components from its H^2 dependence.

This two component analysis enables us to estimate the weight of the superconducting contribution, W_{SC}, for the total quasiparticle tunneling MC. The saturated value of $\Delta\sigma_c^{SC-DOS}$ is given by the y intercepts, A, of the high field H^2-linear behavior as shown in Fig. 2(e). The total quasiparticle contributions, $\Delta\sigma_c^{qp} = \Delta\sigma_c^{SC-DOS} + \Delta\sigma_c^{PG}$, are given by B of the figure. Then, we can estimate $W_{SC} = \Delta\sigma_c^{SC-DOS}/(\Delta\sigma_c^{SC-DOS} + \Delta\sigma_c^{PG})$, by A/B. At 50 K, W_{SC} is estimated as 66% at 55 T. The estimated value is reliable in that it can be obtained directly from the raw MC data. Considering that the data are obtained at T_c, this value is fairly

large. Furthermore, the field at which $\Delta\sigma_c^{SC-DOS}$ saturates is used to determine H_{c2}. Thus H_{c2} is estimated as 41, 22, 13, 12, and 10 T at 50, 60, 65, 70, and 75 K, respectively. However, $\Delta\sigma_c^{PG}$ does not saturate even under high fields up to 55 T. This indicates that the field needed to close the pseudogap, H_{pg} [4], is very high (far greater than 55 T).

Next, we consider $\sigma_c(H)$ below T_c. Here, the $\sigma_c(H)$ behavior [positive $\sigma_c(H)$ slope] above T_c is continuously observed above H_{peak}. However, in this case, as MC does not exhibit H^2 behavior for whole fields, it is difficult to estimate the pseudogap contribution directly from the MC data. Therefore, we assume it from the data above T_c. Figure 3(a) shows the a values obtained in Figs. 2(b)–2(d) for the pseudogap contribution above T_c. The accuracy of the data is not sufficient to determine the precise functional form (either sublinear or superlinear) for the temperature dependence of a. Thus the a value near T_c was simply assumed to be linear in temperature. Note that this is an approximation near T_c to estimate a in the superconducting state. At higher temperatures ($\geqslant 80$ K),
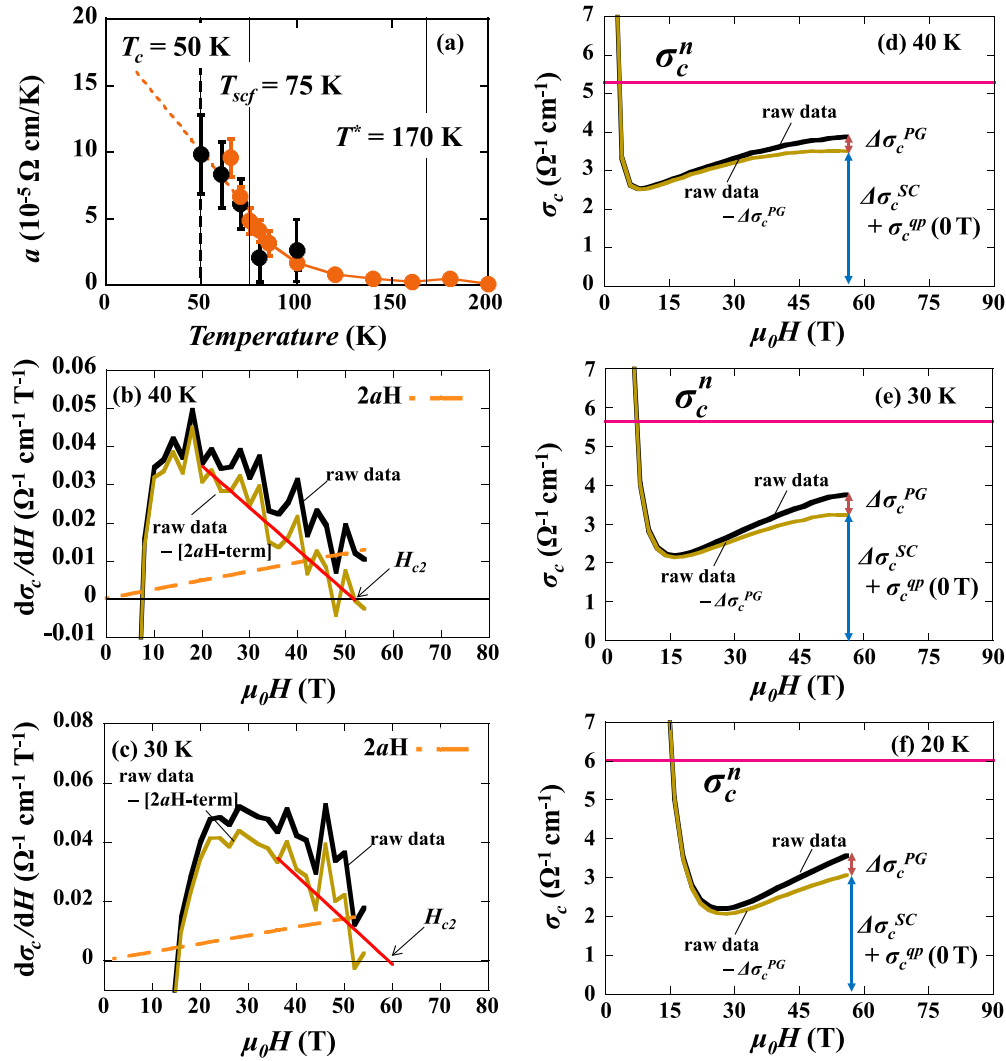
FIG. 3. (a) Temperature dependence of a. Black and orange circles represent the estimation using data of a pulsed magnet [Figs. 2(b) and 2(c)] and of a steady magnet [Fig. 2(d)], respectively (for some data points, the raw MC data were not shown). The dashed line represents a linear extrapolation of the a values. (b), (c) Magnetic field dependences of the raw $d\sigma_c/dH$ data and the pseudogap contribution $(2aH)$-subtracted data for 40 K and 30 K, respectively. The broken lines represent the pseudogap contribution. The solid lines represent linear extrapolations of the subtracted data. (d)–(f) Magnetic field dependence of raw σ_c data and the pseudogap contribution $\Delta\sigma_c^{PG}$-subtracted data at 40, 30, and 20 K, respectively. Here, $\Delta\sigma_c^{SC-DOS} + \sigma_c^{qp}(0\,T)$ corresponds to the subtracted data.

the slope becomes smaller, and the a value approaches zero at around $T^* = 170$ K. Figures 3(b) and 3(c) show the magnetic field dependence of $d\sigma_c/dH$ at 40 and 30 K, respectively. To determine only the superconducting contribution to the data, the above pseudogap contribution is subtracted from the raw data. We find that the pseudogap contribution is not very large. In this case, H_{c2} may correspond to the field at which the superconducting $d\sigma_c/dH$ is extrapolated to zero. Thus H_{c2} is estimated as 51 and 60 T for 40 and 30 K, respectively.

We then investigate the weight of superconducting contribution W_{SC} below T_c. For this purpose, the magnetic field dependences of σ_c and σ_c-$\Delta\sigma_c^{PG}$ are plotted in Figs. 3(d)–3(f) at 40, 30, and 20 K, respectively. At the highest field (55 T), we consider σ_c as σ_c^{qp} because σ_c^{Cooper} may be negligible. Then, σ_c-$\Delta\sigma_c^{PG}$ is expressed as $\Delta\sigma_c^{SC-DOS} + \sigma_c^{qp}(0\,T)$. Assuming

that $\sigma_c^{qp}(0\,T)$ at 20 K is negligible, the result in Fig. 3(f) implies that W_{SC} accounts for $\approx 80\%$ of the total MC. This indicates that the positive slope for the MC primarily originates from superconductivity.

Figure 4 shows the high pulsed magnetic field data for $\rho_{ab}(H)$ at several temperatures above and below T_c. With increasing magnetic fields, $\rho_{ab}(H)$ changes from zero to a resistive state at H_m and rapidly increases in a similar manner as $\rho_c(H)$ [Fig. 2(a)]. It then gradually approaches a constant value, keeping a positive slope. This in-plane behavior contrasts the out-of-plane behavior, in which $\rho_c(H)$ shows a typical negative slope at higher fields, indicating that, in Fig. 2(a), we have succeeded in detecting a property peculiar to $\rho_c(H)$. The superconducting fluctuation theory [10] including the DOS contribution in highly anisotropic materials predicts that, for the out-of-plane conduction, the negative DOS
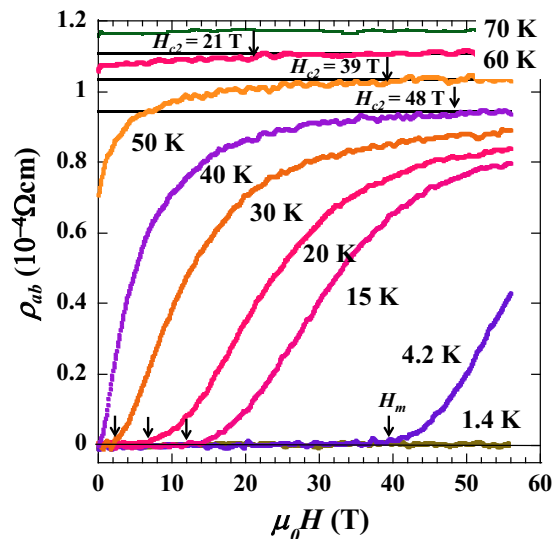
FIG. 4. Magnetic field dependence of ρ_{ab} for $Bi_{1.6}Pb_{0.4}Sr_2$ $CaCu_{1.96}Fe_{0.04}O_{8+\delta}$ at several temperatures above and below T_c. The arrows indicate the upper critical field H_{c2} (H_{c2} is defined as the field at which ρ_{ab} decreases 1% from the high field constant value), and the vortex melting field H_m (H_m is defined as a field in which $\rho_{ab} = 0.01\rho_{ab}^n$).
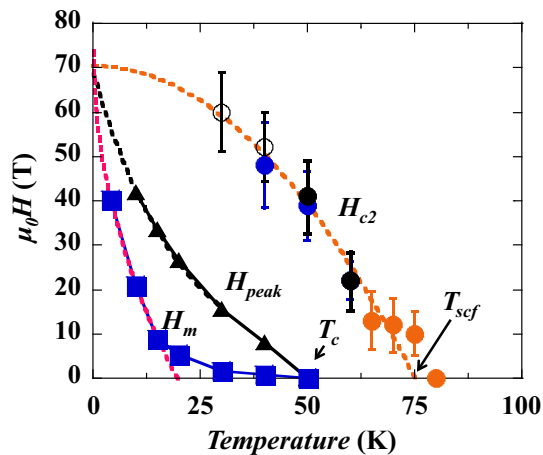

FIG. 5. Characteristic fields versus temperature. The melting field H_m, peak field H_{peak}, and upper critical field H_{c2} are shown as solid squares, solid triangles, and circles, respectively. The H_{c2} data points represented by black solid circles, blue solid circles, orange solid circles, and black open circles have been determined in Figs. 2(b), 2(c), 4, 2(d), 3(b), and 3(c), respectively. Here, an open symbol indicates that the data were obtained by extrapolation. The dashed lines are numerical fits for each field (see text).

contribution dominates over the positive Aslamazov-Larkin (AL) contribution near H_{c2}, resulting in a negative slope for $\rho_c(H)$. For the in-plane conduction, the AL contribution dominates, causing the positive slope for $\rho_{ab}(H)$. The experimental observations in this study are consistent with this theory. Then, it may be natural to ascribe the origin of the negative $\rho_c(H)$ slope (positive slope for the out-of-plane MC) primarily to the superconducting DOS fluctuation effect. Supposing that $\rho_{ab}(H)$ is constant above H_{c2}, H_{c2} is estimated as 21, 39, and 48 T for 60, 50, and 40 K, respectively. These values agree with those obtained by $\rho_c(H)$ measurements, supporting the validity of the above analysis for $\rho_c(H)$.

Figure 5 shows H_m, H_{peak}, and H_{c2} obtained by $\rho_c(H)$ measurements as well as H_{c2} obtained by $\rho_{ab}(H)$ measurements as a function of temperature. In highly two-dimensional (2D) superconductors such as high-T_c cuprates, the vortex system transforms from a liquid state to a 2D solid state upon cooling [18]. The transition temperature is represented as T_m^{th}. Here, the field at which the vortex melting line extrapolates to 0 K is simply considered to be $H_{c2}(0)$ at $T = 0$. To estimate $H_{c2}(0)$, we adopted the 2D vortex solid state formula, $T_m^{th}/T_c = (c_L^2/Gi^{2D})[1 - H/H_{c2}(0)]^2$ [18]. Here, we tentatively used the same parameter values, namely the Ginzburg number $Gi^{2D} = 0.05$ and the Lindemann number $c_L = 0.14$, as in the previous report [5] with the exception of $T_c(=50\,K)$. The fitting to the experimental data is very good between 4.2 K and 15 K, probably better than that of Ref. [5], and the fitting gives $H_{c2}(0) = 70\,T$. The extrapolation of H_{peak} to 0 K gives $H_{peak} = 69\,T$; here, we assumed H_{peak} at low temperatures is exponential in T [4]. On the other hand, $H_{c2}(0)$ is directly estimated as 70 T by fitting the obtained $H_{c2}(T)$ using the empirical formula $H_{c2}(T) = H_{c2}(0)[1 - (T/T_c)^2]$; here, we assumed the T_{scf} value (=75 K)

for T_c. All three superconductivity-related characteristic fields roughly coincide at $T = 0$, indicating that the obtained $H_{c2}(T)$ contain information on the upper critical field. Hence the above procedure (two component analysis in MC) for estimating $H_{c2}(T)$ from $\rho_c(H)$ data should be appropriate. In superconductors with strong fluctuation, the mean-field upper critical field, H_0, and the mean-field superconducting transition temperature in $H = 0$, T_0, are shown to be the onset of superconducting fluctuation [19] (see Fig. 3 in Ref. [19]). We consider that H_{c2} and T_{scf} in this study correspond to H_0 and T_0, respectively.

In a pioneering report [5], an unconventionally large quantum-dissipative pseudogapped state was shown to exist near $T = 0$. However, we did not observe such behavior in our sample (Fig. 5). Note that H_m is not observed until 55 T at 1.4 K [Figs. 2(a) and 4]. We assume that our sample acquired a strong vortex pinning effect through the codoping of Pb and Fe, and thus such anomalous behavior has been suppressed compared to that in the pristine Bi-2212 sample of Ref. [5].

Finally, we briefly discuss the implication of our result on the pseudogap problem. In this study, we have revealed that the superconducting contribution to the positive slope for the out-of-plane MC evolves below T_{scf} in addition to the pseudogap contribution. This result, on one hand, confirms that the pseudogap and superconductivity are distinct, as many authors suggest [20–22]. On the other hand, this result verifies that superconductivity is another cause for the anomalous $\rho_c(T,H)$ behavior. Recently, we have observed a pseudogaplike upturn and negative MR in $\rho_c(T,H)$ just above T_c for heavily overdoped Bi-2212 ($p = 0.23$) [13]. Thus this behavior should be attributed to superconductivity; the pseudogap does not open above T_c in this doping state. Therefore, if we could know whether or

not the pseudogap opens below T_c in this heavily overdoped sample, we would understand the pseudogap phase diagram completely.

IV. CONCLUSIONS

In summary, to determine the origin of the positive slope in interlayer MC in high-T_c cuprates, $\rho_c(T,H)$ as well as $\rho_{ab}(T,H)$ measurements under high pulsed magnetic fields were performed on Pb and Fe codoped Bi-2212. The results not only establish that the positive MC and the correlated upturn for $\rho_c(T)$ near T_c are a sign of superconductivity but also enable us to estimate H_{c2} and the superconducting contribution on the positive MC

quantitatively. This finding may provide an important clue toward understanding the pseudogap phenomenon in high-T_c superconductivity.

[1] B. Keimer, S. A. Kivelson, M. R. Norman, S. Uchida, and J. Zaanen, Nature (London) **518**, 179 (2015).

[2] H. Alloul, F. Rullier-Albenque, B. Vignolle, D. Colson, and A. Forget, Europhys. Lett. **91**, 37005 (2010).

[3] T. Watanabe, T. Fujii, and A. Matsuda, Phys. Rev. Lett. **84**, 5848 (2000).

[4] T. Shibauchi, L. Krusin-Elbaum, M. Li, M. P. Maley, and P. H. Kes, Phys. Rev. Lett. **86**, 5763 (2001).

[5] T. Shibauchi, L. Krusin-Elbaum, G. Blatter, and C. H. Mielke, Phys. Rev. B **67**, 064514 (2003).

[6] A. Yurgens, D. Winkler, N. V. Zavaritsky, and T. Claeson, Phys. Rev. Lett. **79**, 5122 (1997).

[7] A. N. Lavrov, Y. Ando, and S. Ono, Europhys. Lett. **57**, 267 (2002).

[8] N. Morozov, L. Krusin-Elbaum, T. Shibauchi, L. N. Bulaevskii, M. P. Maley, Y. I. Latyshev, and T. Yamashita, Phys. Rev. Lett. **84**, 1784 (2000).

[9] K. E. Gray and D. H. Kim, Phys. Rev. Lett. **70**, 1693 (1993).

[10] A. A. Varlamov, G. Balestrino, E. Milani, and D. V. Livanov, Adv. Phys. **48**, 655 (1999).

[11] V. M. Krasnov, A. E. Kovalev, A. Yurgens, and D. Winkler, Phys. Rev. Lett. **86**, 2657 (2001).

[12] S. D. Obertelli, J. R. Cooper, and J. L. Tallon, Phys. Rev. B **46**, 14928 (1992).

[13] T. Usui, D. Fujiwara, S. Adachi, H. Kudo, K. Murata, H. Kushibiki, T. Watanabe, K. Kudo, T. Nishizaki, N. Kobayashi, S. Kimura, K. Yamada, T. Naito, T. Noji, and Y. Koike, J. Phys. Soc. Jpn. **83**, 064713 (2014).

[14] T. Watanabe, T. Fujii, and A. Matsuda, Phys. Rev. Lett. **79**, 2113 (1997).

[15] T. Usui, S. Adachi, T. Watanabe, and T. Nishizaki, Phys. Proc. **65**, 49 (2015).

[16] K. Kadowaki, Physica C **263**, 164 (1996).

[17] A. E. Koshelev, Phys. Rev. Lett. **76**, 1340 (1996).

[18] G. Blatter, M. V. Feigel'man, V. B. Geshkenbein, A. I. Larkin, and V. M. Vinokur, Rev. Mod. Phys. **66**, 1125 (1994).

[19] R. Ikeda, J. Phys. Soc. Jpn. **72**, 2930 (2003).

[20] V. M. Krasnov, A. Yurgens, D. Winkler, P. Delsing, and T. Claeson, Phys. Rev. Lett. **84**, 5860 (2000).

[21] M. Suzuki and T. Watanabe, Phys. Rev. Lett. **85**, 4787 (2000).

[22] K. Tanaka, W. S. Lee, D. H. Lu, A. Fujimori, T. Fujii, I. Risdiana, I. Terasaki, D. J. Scalapino, T. P. Devereaux, Z. Hussain, and Z.-X. Shen, Science **314**, 1910 (2006).